

Rapid #: -20865746

CROSS REF ID: 1319344

LENDER: CUV (Univ. of California, Davis) :: Shields Library

BORROWER: NRC (North Carolina State Univ.) :: Main Library

TYPE: Article CC:CCG

JOURNAL TITLE: International journal for uncertainty quantification

USER JOURNAL TITLE: INTERNATIONAL JOURNAL FOR UNCERTAINTY QUANTIFICATION

ARTICLE TITLE: GLOBAL SENSITIVITY ANALYSIS OF RARE EVENT PROBABILITIES USING SUBSET

SIMULATION AND POLYNOMIAL CHAOS EXPANSIONS

ARTICLE AUTHOR: Merritt, Michael

VOLUME: 13

ISSUE: 1

MONTH:

YEAR: 2023

PAGES: 53-67

ISSN: 2152-5080

OCLC #:

Processed by RapidX: 6/7/2023 12:08:05 PM

This material may be protected by copyright law (Title 17 U.S. Code)

GLOBAL SENSITIVITY ANALYSIS OF RARE EVENT PROBABILITIES USING SUBSET SIMULATION AND POLYNOMIAL CHAOS EXPANSIONS

Michael Merritt,^{1,*} Alen Alexanderian,¹ & Pierre Gremaud²

¹Department of Mathematics, NC State University, Raleigh, North Carolina 27695-8205, USA ²The Graduate School and Department of Mathematics, NC State University, Raleigh, North Carolina 27695-7102, USA

*Address all correspondence to: Michael Merritt, Department of Mathematics, NC State University, Raleigh, North Carolina 27695-8205, USA, E-mail: mbmerrit@ncsu.edu

Original Manuscript Submitted: 5/19/2021; Final Draft Received: 6/12/2022

By their very nature, rare event probabilities are expensive to compute; they are also delicate to estimate as their value strongly depends on distributional assumptions on the model parameters. Hence, understanding the sensitivity of the computed rare event probabilities to the hyper-parameters that define the distribution law of the model parameters is crucial. We show that by (i) accelerating the calculation of rare event probabilities through subset simulation and (ii) approximating the resulting probabilities through a polynomial chaos expansion, the global sensitivity of such problems can be analyzed through a double-loop sampling approach. The resulting method is conceptually simple and computationally efficient; its performance is illustrated on a subsurface flow application and on an analytical example.

KEY WORDS: global sensitivity analysis, rare event simulation, polynomial chaos, high-dimensional methods

1. INTRODUCTION

Quantifying rare event probabilities is often needed when modeling under uncertainty [1–4]. Rare events are commonly associated with system failures or anomalies which pose a risk; it is thus imperative that rare event probabilities be computed reliably. For the sake of concreteness, we consider q to be a scalar-valued quantity of interest (QoI) whose inputs are drawn from the sample space $\Theta \subseteq \mathbb{R}^d$ with associated sigma algebra \mathcal{F} and probability measure \mathbb{P} . For a given threshold $\bar{\tau}$, the corresponding rare event probability is defined as

$$P_{\bar{\tau}} = \mathbb{P}(q(\mathbf{\theta}) > \bar{\tau}),\tag{1}$$

where $\theta \in \Theta$ is a random vector whose entries represent uncertain model parameters. Rare event probabilities are notoriously challenging to compute; indeed, basic Monte Carlo simulations of Eq. (1) are inefficient in this context for the simple reason that few samples actually hit the rare event domain. Several methods have been proposed to compute $P_{\bar{\tau}}$ more efficiently, ranging from importance sampling and Taylor series approximations to subset simulation, the latter of which we use in this article; see for instance [3] and Section 3.

The evaluation of the rare event probability (1) requires the distribution law governing the model parameters θ . In practice, such a law is typically *assumed*. Clearly, $P_{\overline{\tau}}$ depends on these assumptions; should they be misguided, the resulting rare event probability is likely be misleading. We let ξ denote a set of hyper-parameters characterizing the distribution law of θ . It is crucial to understand the sensitivity of $P_{\overline{\tau}}$ to ξ . In this article, we develop an efficient method to quantify, through global sensitivity analysis (GSA), the robustness of $P_{\overline{\tau}}$ to the choice of hyper-parameters characterizing the distribution law of the model parameters. To account for the uncertainty in ξ , we model the corresponding hyper-parameters as random variables. The rare event probability takes the form

$$P_{\bar{\tau}}(\xi) = \mathbb{P}(\{q(\theta) > \bar{\tau}\} \mid \xi). \tag{2}$$

For a generic QoI $p(\xi)$, GSA aims at ascribing to any entry of ξ (or any group of entries) its relative "importance" in determining p; the importance measures built within GSA do not just consider p locally at a given ξ^* (as in local sensitivity analysis) but instead take into account the full range of values ξ . In their simplest form, Sobol' indices [5–8] attach to each entry of ξ its relative contribution to the variance of p. In other words, in the context of Sobol' indices, the variance is taken as a proxy for uncertainty; the approach benefits from the nice algebraic properties of the variance and can be derived from the ANOVA decomposition of p. GSA using Sobol' indices has been utilized in a wide range of applications such as porous media flow [9–11], ocean modeling [12,13], chemical kinetics [14–16], epidemiology [17,18], and neuroscience [19], to name a few; see also, [20, Chap. 6], for a list of applications. For a generic QoI, computing Sobol' indices requires costly Monte Carlo integrations; the associated costs are a significant bottleneck of the approach. To increase their range of applicability, Sobol' indices are often applied in practice to a surrogate \hat{p} of p where \hat{p} is chosen such that its indices can be computed cheaply (or for free); this is the approach we use below. We refer the reader to [21] for more background on GSA.

A number of recent studies have considered how to assess the sensitivity of rare event estimation procedures to uncertain inputs and/or to the distributions of these inputs. There is a general consensus that the naive double-loop approach—whereby for each realization of ξ multiple samples of θ are used to estimate $P_{\bar{\tau}}$ —is infeasible but for the simplest of problems. An early work [4] combines rare event estimation techniques with the traditional Monte Carlo approach for GSA of the hyper-parameters. Several studies introduce new sensitivity measures [22–25] which are tailored to make the rare event SA process more tractable. Others perform sensitivity analysis in the joint space of both input parameters and hyper-parameters [22,25–27]. These methods increase computational efficiency through use of local SA methods [22], surrogate models [25], kernel density estimates [26], and kriging [27]. A thorough overview of current methods at the intersection of SA and rare event simulation can be found in [28].

Our main contribution is to show that a double-loop approach can in fact be not only feasible but computationally expedient in order to perform GSA of $P_{\bar{\tau}}(\xi)$ with respect to ξ . This may seem counterintuitive since, while informative, this type of second level sensitivity analysis is expensive. We propose an approach that addresses this challenge through a combination of fast methods for rare event simulations together with the use of surrogate models. Specifically, we rely on subset simulation [3] to estimate rare event probabilities and approximate $P_{\bar{\tau}}(\xi)$ using a polynomial chaos expansion (PCE); see, respectively, in Sections 3 and 4. GSA is performed through a variance-based approach: crucially, the Sobol' indices for appropriate approximations to $P_{\bar{\tau}}(\xi)$ can then be obtained "for free" through analytical formulæ. By using sparse regression to construct the PCE, our approach is able to perform accurate GSA of the rare event probability, while mitigating the noise incurred from inexpensive approximations of $P_{\bar{\tau}}(\xi)$. As an added benefit, our approach is structurally simpler than most of the previously cited work.

To demonstrate the efficiency gains of the proposed method, we present an illustrative example in Section 2 and deploy our approach on it in Section 5.1. In Section 5.2, we apply the method to a Darcy flow problem requiring multiple estimates of the rare event probability to show feasibility in a more computationally demanding framework. We discuss additional challenges, perspectives and future work in Section 6.

2. A MOTIVATING EXAMPLE

We consider the following illustrative example [3,29,30] throughout the article,

$$q(\mathbf{\theta}) = -\frac{1}{\sqrt{d}} \sum_{i=1}^{d} \mathbf{\theta}_i, \tag{3}$$

where q is the QoI in Eq. (1) and $\theta = \begin{bmatrix} \theta_1 \dots \theta_d \end{bmatrix}^\top$ with independent normally distributed entries $\theta_i \sim \mathcal{N}(\mu_i, \sigma_i^2)$, $i = 1, \dots, d$. It is elementary to check that, for any values of the hyper-parameters $\boldsymbol{\xi} = \begin{bmatrix} \mu_1 \dots \mu_d & \sigma_1^2 \dots \sigma_d^2 \end{bmatrix}^\top$,

$$q \sim \mathcal{N}(\bar{\mu}, \bar{\sigma}^2) \quad \text{with} \begin{cases} \bar{\mu} = -\frac{1}{\sqrt{d}} \sum_{i=1}^d \mu_i \\ \bar{\sigma}^2 = \frac{1}{d} \sum_{i=1}^d \sigma_i^2 \end{cases}$$
 (4)

For a given ξ , the rare event probability is simply

$$P_{\bar{\tau}}(\xi) = \frac{1}{2} - \frac{1}{2} \operatorname{erf}\left(\frac{\bar{\tau} - \bar{\mu}}{\sqrt{2}\bar{\sigma}}\right). \tag{5}$$

We model the uncertainty in the hyper-parameters by considering them as independent uniformly distributed random variables with a 10% perturbation around their respective nominal values. Figure 1 illustrates the case d=5 with $\xi_{nom}=\begin{bmatrix}1&2&3&4&5&10&8&6&4&2\end{bmatrix}^{\top}$ as the nominal value for ξ . In particular, Fig. 1, right, shows how the uncertainty in $P_{\bar{\tau}}$ changes as $\bar{\tau}$ varies. As $\bar{\tau}$ increases, i.e., as the event becomes rarer, the uncertainty in $P_{\bar{\tau}}$ —measured through its coefficient of variation—increases. We contend that this latter behavior is generic for rare event simulations, establishing the need for methods allowing the quantification of the effects of hyper-parameter choices on the uncertainty in $P_{\bar{\tau}}$.

To provide qualitative insight, we present a rough estimate for the decrease in the coefficient of variation of $P_{\bar{\tau}}$, as the event becomes less rare. We consider a generic $P_{\bar{\tau}}(\xi)$ as defined in Eq. (2) and assume $P_{\bar{\tau}}$ is a random variable (i.e., a measurable function of ξ). Let $\mu = \mathbb{E}(P_{\bar{\tau}})$ and $\sigma^2 = \mathbb{V}(P_{\bar{\tau}})$ be the mean and variance of $P_{\bar{\tau}}$. Recall that the coefficient of variation of $P_{\bar{\tau}}$ is given by $\delta(P_{\bar{\tau}}) = \sigma/\mu$. Note that for every ξ , we have $0 \leq P_{\bar{\tau}}(\xi) \leq 1$; thus, $P_{\bar{\tau}}(\xi) \geq P_{\bar{\tau}}(\xi)^2$ and

$$\sigma^2 = \mathbb{E}(P_{\bar{\tau}}^2) - \mu^2 \le \mu - \mu^2 = \mu(1 - \mu). \tag{6}$$

Therefore, $\delta^2(P_{\bar{\tau}}) = \sigma^2/\mu^2 \le \mu(1-\mu)/\mu^2 = (1-\mu)/\mu$. Note that as the event becomes less rare, μ will grow resulting in the diminishing of the bound on the coefficient of variation. We point out that the inequality (6) can be obtained directly from the more general Bhatia–Davis inequality [31].

3. RARE EVENT SIMULATION

Monte Carlo simulation is a standard way of approximating the rare event probability $P_{\bar{\tau}}$ defined in Eq. (1). Observe that

$$P_{\bar{\tau}} = \mathbb{E}[\chi_{\bar{\tau}}] = \int_{\Theta} \chi_{\bar{\tau}}(\boldsymbol{\theta}) \pi(\boldsymbol{\theta}) d\boldsymbol{\theta}, \tag{7}$$

where $\chi_{\bar{\tau}}$ denotes the indicator function of the set $\{\theta \in \Theta : q(\theta) > \bar{\tau}\}$ and $\pi(\theta)$ is the PDF of θ . This leads to the following Monte Carlo (MC) estimator,

$$\hat{P}_{\bar{\tau}}^{\text{MC}} = \frac{1}{N} \sum_{i=1}^{N} \chi_{\bar{\tau}}(\boldsymbol{\theta}^{(i)}), \tag{8}$$

where $\theta^{(i)}$, i = 1, ..., N, are (independent) realizations of θ .

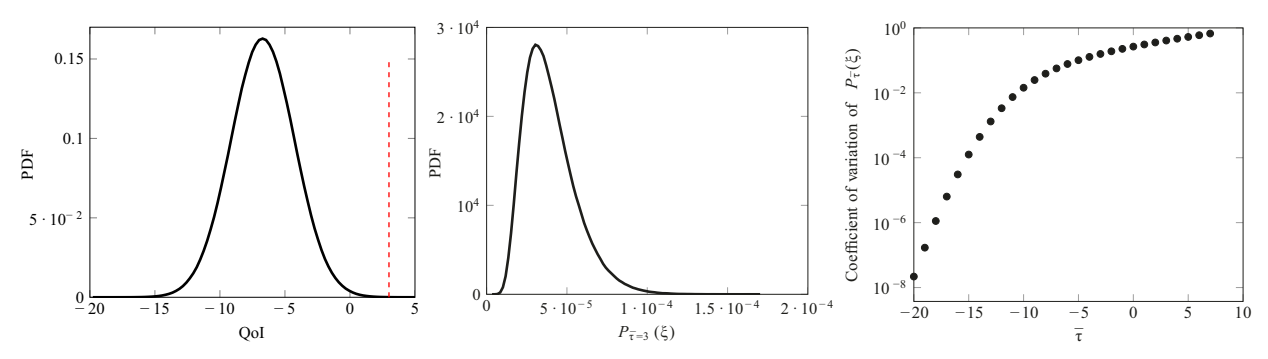


FIG. 1: Left: Probability distribution function (PDF) of q from Eq. (3) with the rare event threshold $\bar{\tau}=3$ indicated by a vertical line; middle: PDF of $P_3(\xi)$; note that from Eq. (5), $P_3(\xi_{nom})\approx 3.69\times 10^{-5}$; right: coefficient of variation of $P_{\bar{\tau}}(\xi)$ (ratio of standard deviation to mean) as $\bar{\tau}$ varies

In the case of rare events, i.e., of small probabilities $P_{\bar{\tau}}$, the basic MC estimator (8) becomes computationally inefficient. Indeed, consider the coefficient of variation $\delta(\hat{P}_{\bar{\tau}}^{\text{MC}})$ of the above estimator and observe

$$\delta^{2}\left(\hat{P}_{\bar{\tau}}^{\mathrm{MC}}\right) = \frac{\mathbb{V}\left(\hat{P}_{\bar{\tau}}^{\mathrm{MC}}\right)}{\mathbb{E}\left[\hat{P}_{\bar{\tau}}^{\mathrm{MC}}\right]^{2}} = \frac{1 - P_{\bar{\tau}}}{NP_{\bar{\tau}}} \approx \frac{1}{NP_{\bar{\tau}}} \quad \text{if } 0 < P_{\bar{\tau}} \ll 1.$$

$$\tag{9}$$

In other words, ensuring a given accuracy requires $N \approx 1/(P_{\bar{\tau}}\delta^2)$. For increasingly rare events, i.e., small $P_{\bar{\tau}}$, the error in Eq. (8) will increase accordingly. Standard MC methods are thus poor candidates for rare event estimation.

3.1 The Subset Simulation Method

We rely on the subset simulation (SS) method [32,33] to accelerate rare event computation. This approach decomposes the rare event estimation problem into a series of "frequent event" estimation problems that are more tractable; it has been observed that this may reduce the coefficient of variation by more than an order of magnitude over standard MC [3,32,33]. This corresponds to a substantially lower computational burden for estimating rare event probabilities.

Consider the rare event domain $F = \{ \theta \in \Theta \mid q(\theta) > \bar{\tau} \}$ and a sequence of nested subsets of F,

$$F = F_L \subset \cdots \subset F_2 \subset F_1$$

where $F_i = \{\theta \in \Theta \mid q(\theta) > \tau_i\}, i = 1, ..., L$ with $\tau_1 < \tau_2 < \cdots < \tau_L = \bar{\tau}$. The rare event probability $P_{\bar{\tau}}$ can thus be decomposed into a product of conditional probabilities,

$$P_{\bar{\tau}} = \mathbb{P}(F) = \mathbb{P}\left(\bigcap_{i=1}^{L} F_i\right) = \prod_{i=1}^{L} \mathbb{P}(F_i \mid F_{i-1}), \tag{10}$$

with, by convention, $F_0 = \Theta$. Computing $P_{\bar{\tau}}$ according to Eq. (10) requires an efficient and accurate method for estimating the L conditional probabilities. We use a modification of the Metropolis-Hastings algorithm to accomplish this [32]. This modified Metropolis algorithm (MMA), which belongs to the family of Markov chain Monte Carlo (MCMC) methods, draws samples from a conditional distribution and either accepts or rejects the samples based on a chosen acceptance parameter. One uses samples that belong to F_{i-1} as seeds for estimating the conditional probability $\mathbb{P}(F_i|F_{i-1})$. We refer the interested reader to [3], which provides a high level discussion of MMA as well as other variants of SS; a more thorough analysis of MMA and MCMC algorithms can be found in [30].

Choosing a proper sequence of thresholds $\{\tau_i\}_{i=1}^L$ is a major challenge of the SS method. Since one has little prior knowledge of the PDF of $q(\theta)$, it is often not feasible to prescribe the sequence of thresholds *a priori*. Instead, one may require that $\mathbb{P}(F_i \mid F_{i-1}) = p_0$, $i = 1, \ldots, L-1$, for some chosen quantile probability p_0 [32]. We can then iteratively estimate the proper threshold at each "level" of the algorithm; the SS estimator of Eq. (10) takes the form

$$P_{\bar{\tau}} \approx \hat{P}_{\bar{\tau}}^{SS} = p_0^{L-1} \, \mathbb{P}(F_L \mid F_{L-1}),$$
 (11)

where the final conditional probability $\mathbb{P}(F_L \mid F_{L-1})$ is estimated via the MMA procedure mentioned earlier. Although $p_0 = 0.1$ is a standard choice in engineering applications, there has been significant work done to determine optimal values for p_0 ; this, in general, depends on the QoI under consideration. It has been shown that, for practical purposes, the optimal p_0 lies in the interval [0.1, 0.3] and that, within this interval, the efficiency of SS is insensitive to the particular choice of p_0 [34]. With the approach for computing the sequence of thresholds in Eq. (10), each τ_i is a random variable, estimated via a finite number of conditional samples. Consequently the number of levels or iterations necessary to terminate SS is also random. For a sufficiently large number of samples, the number of levels is given in [29] as

$$L - 1 = \left\lfloor \frac{\log P_{\bar{\tau}}}{\log p_0} \right\rfloor. \tag{12}$$

3.2 Implementation of Subset Simulation

For completeness, we provide an algorithm outline for the SS method in Algorithm 1. We assume Gaussian inputs in the examples considered in this article; the SS method can, however, be applied to non-Gaussian input distributions; see Appendix B of [35] for details. Additional information on the implementation of the SS algorithm, including the MMA implementation, is, for instance, available in [1,29,32]. As this MCMC implementation reuses the input parameters from each previous level to estimate the threshold for the next level, this method does not require any burn-in samples to draw from the conditional distribution; it begins by sampling from the previous rare event domain. On the theoretical side, the SS algorithm is asymptotically unbiased and $\hat{P}_{\bar{\tau}}^{SS}$ converges almost surely to the true rare event probability, $P_{\bar{\tau}}$. For a detailed convergence analysis of SS and derivation of its statistical properties, see [32].

3.3 Computational Cost

We turn now to the computational cost of estimating $P_{\bar{\tau}}$ using SS. The computational cost is measured in terms of the number of function evaluations required to run the algorithm. As the number of levels L is random, so is the computational cost associated with SS. For simplicity, we assume for our cost analysis that a sufficient number of samples has been used so that L does not vary. The total number of QoI evaluations required by SS is $L \cdot N_{\rm SS}$, where $N_{\rm SS}$ is a user-defined parameter that determines the number of samples per intermediate level of the iteration. Say, for example, the true rare event probability is 10^{-6} and we wish to estimate $P_{\bar{\tau}}$ with a coefficient of variation within $\delta = 0.1$. For standard MC sampling, we would need $N \geq 1/(\delta^2 \cdot P_{\bar{\tau}}) = 10^8$ samples of the QoI. Take the SS method with a quantile probability of $p_0 = 0.1$. Then, according to Eq. (12), we would have L = 7, corresponding to seven levels of conditional probabilities. The coefficient of variation for each of the conditional probabilities is more difficult to quantify, however, as in the case of the standard MC estimator, they are proportional to $1/p_0$; see [32]. In this case, one would expect to see a significant reduction in the cost of estimating $P_{\bar{\tau}}$ with SS.

We lastly emphasize the power of SS for estimating rare event probabilities in the context of QoIs with high-dimensional inputs. Not only does SS improve upon the slow convergence rates of standard MC by a wide margin, it also inherits the property of having a convergence rate independent of input dimension.

4. SURROGATES FOR GSA OF RARE EVENT PROBABILITIES

We seek to apply variance-based GSA to $P_{\bar{\tau}}(\xi)$, defined in Eq. (2), with respect to components of ξ . To mitigate the computational expense of performing such analysis, we combine the SS algorithm and surrogate models, in the form

```
Algorithm 1: Subset simulation
    Input: Rare event threshold, \bar{\tau}; samples per level, N_{SS}; quantile probability, p_0; routine that evaluates QoI, q(\theta)
    Output: Estimate of rare event probability: \hat{P}_{\bar{\tau}}^{SS}
 1 Draw N_{\rm SS} samples of \theta from appropriate distribution
 2 Compute N_{SS} samples of the QoI; compute \tau_1 as the p_0 quantile
 3 Save the |N_{SS} \cdot p_0| inputs such that q(\theta) > \tau_1 as seeds for the next level
                                                                                  // i indicates the current level
 5 while \tau_i < \bar{\tau} do
         i \leftarrow i + 1
         Sample \theta by creating \lfloor N_{\rm SS} \cdot p_0 \rfloor Markov Chains, each with length \lfloor p_0^{-1} \rfloor // For details, see [32]
 7
         Using MCMC seeds, evaluate the QoI and compute \tau_i as the p_0 quantile
         Save the \lfloor N_{\rm SS} \cdot p_0 \rfloor inputs such that q(\theta) > \tau_i as seeds for the next level
10 end
11 Using seeds from F_{L-1}, sample the QoI and estimate \mathbb{P}(F_L \mid F_{L-1}) using MC
12 Evaluate \hat{P}^{\mathrm{SS}}_{ar{	au}} = p^i_0 \ \mathbb{P}(F_L \mid F_{L-1})
```

of polynomial chaos expansions (PCEs). We assume ξ to be an M-dimensional vector with independent entries. The procedure, which amounts to double-loop sampling, is outlined below:

- ullet Generate hyper-parameter samples $\{\mathbf{\xi}^{(j)}\}_{j=1}^{N_{\mathrm{SAMP}}}$.
- For each $j \in \{1, \dots, N_{\text{SAMP}}\}$, estimate $P_{\bar{\tau}}(\boldsymbol{\xi}^{(j)})$ using SS; denote these estimates by $P_{\bar{\tau}}^{(j)} = \text{SS}(P_{\bar{\tau}}(\boldsymbol{\xi}^{(j)}))$.
- Use the (noisy) function evaluations $\{P_{\bar{\tau}}^{(j)}\}_{j=1}^{N_{\text{SAMP}}}$ to compute a surrogate model $\tilde{P}_{\bar{\tau}}(\xi) \approx P_{\bar{\tau}}(\xi)$.
- Compute the Sobol' indices of $\tilde{P}_{\bar{\tau}}(\xi)$.

Instead of using SS for computing $P_{\bar{\tau}}(\xi^{(j)})$, one may be tempted to apply a surrogate further "upstream" by computing a surrogate model $\tilde{q}_{\xi^{(j)}}(\theta)$ for $q(\theta)$ from samples $\{q(\theta^{(k)})\}_{k=1}^n$ drawn from the law of θ as determined by $\xi^{(j)}$. This surrogate model of q can then be used for fast approximation of the rare event probability $P_{\bar{\tau}}(\xi^{(j)})$. This procedure, however, has two major pitfalls: (i) an expensive surrogate modeling procedure must be carried out for each $j \in \{1, \dots, N_{\text{SAMP}}\}$ and, more importantly, (ii) surrogate models are typically poorly suited to the task of rare event estimation. Indeed, surrogates typically fail to capture the tail behavior of the distribution of the QoI q, making them unsuitable for rare event simulations. This shortcoming is well-documented in the uncertainty quantification literature [36,37] although efforts are being made to tailor the surrogate model construction process for the efficient estimation of rare event probabilities [37–42].

4.1 PCE Surrogate for Rare Event Probability

Our approach leverages the properties of PCE surrogates for fast estimation of Sobol' indices [43,44]; it also takes advantage of the regularity of the mapping $\xi \mapsto P_{\bar{\tau}}(\xi)$. Specifically, assuming the PDF of ξ satisfies certain (mild) differentiability and integrability conditions, one can show that $P_{\bar{\tau}}(\xi)$ is a differentiable function of ξ ; see [45, Proposition 3.5].

The PCE of $P_{\bar{\tau}}(\xi)$ is defined as

$$\tilde{P}_{\bar{\tau}}(\xi) = \sum_{k=0}^{N_{PC}} \beta_k \Psi_k(\xi), \tag{13}$$

where $\Psi_0, \ldots, \Psi_{N_{PC}}$ belong to a family of orthogonal polynomials and $\beta_0, \ldots, \beta_{N_{PC}}$ are the (scalar) PCE coefficients. The specific family of polynomials is chosen to guarantee orthogonality with respect to the PDF of ξ ; see, e.g., [43]. We use a total order truncation scheme for the PCE: the multivariate polynomial basis contains all possible polynomial basis elements up to a total polynomial order r. In this case, N_{PC} in Eq. (13) satisfies

$$N_{PC} + 1 = \frac{(M+r)!}{M!r!}.$$

The coefficients $\beta_0,\ldots,\beta_{N_{PC}}$ can be computed in a number of ways, including nonintrusive spectral projection or regression [43,44,46]. A regression-based approach is preferred here because the evaluations of $P_{\bar{\tau}}$ are noisy due to sampling errors incurred in the SS procedure. We estimate the vector $\boldsymbol{\beta} = [\beta_0,\beta_1,\ldots,\beta_{N_{PC}}]$ from function evaluations $P_{\bar{\tau}}^{(j)} = SS(P_{\bar{\tau}}(\boldsymbol{\xi}^{(j)})), j=1,\ldots,N_{SAMP}$, by solving the penalized least-squares problem:

$$\min_{\beta} \sum_{j=1}^{N_{\text{SAMP}}} \left[P_{\bar{\tau}}^{(j)} - \sum_{k=0}^{N_{\text{PC}}} \beta_k \Psi_k(\boldsymbol{\xi}^{(j)}) \right]^2 \quad \text{s.t.} \quad ||\boldsymbol{\beta}||_1 \le \lambda.$$
 (14)

In Eq. (14), the penalty parameter λ acts as a sparsity control on the recovered PCE coefficients. We generate the realizations $\{\xi^{(j)}\}_{j=1}^{N_{SAMP}}$ of the hyper-parameter vector through Latin hypercube sampling; for further details on the implementation of sparse regression for PCE; see [47,48]. The numerical results in Section 5 are obtained using the SPGL1 solver [49].

4.2 GSA of $P_{\bar{\tau}}$ Using the PCE Surrogate

As is well-known, the Sobol' indices of a PCE surrogate can be computed analytically. For example, the first-order Sobol' indices, $S_i(P_{\bar{\tau}})$, $i=1,\ldots,M$, of $P_{\bar{\tau}}$ can be approximated as follows:

$$S_i(P_{\bar{\tau}}) \approx S_i(\tilde{P}_{\bar{\tau}}) = \frac{\sum_{k \in K_i} \beta_k^2 \mathbb{E}[\Psi_k^2]}{\sum_{k=1}^{N_{\text{PC}}} \beta_k^2 \mathbb{E}[\Psi_k^2]},\tag{15}$$

where K_i denotes the set of all PCE terms that depend only on ξ_i . Sobol' indices for arbitrary subsets of variables, as well as total indices, can be computed in an analogous manner [43,50]. In practice, PCE surrogates with modest accuracy are often sufficient to obtain reliable estimates of Sobol' indices.

While the above approach for GSA of $P_{\bar{\tau}}$ does require repeated simulations of the QoI q during the calls to the SS algorithm, it still provides orders of magnitude speedup over the standard "pick and freeze" MC methods, also known as Saltelli sampling, for computing the Sobol' indices of $P_{\bar{\tau}}$ [51]. Indeed, a fixed sample $\{\xi^{(j)}\}_{j=1}^{N_{\text{SAMP}}}$ with modest N_{SAMP} is sufficient to compute the PCE surrogate from which the Sobol' indices can be computed at a negligible computational cost. Moreover, the sparse regression approach for estimating PCE coefficients is forgiving of noisy function evaluations. Therefore, large sample sizes are not needed in the calls to the SS algorithm. We demonstrate the merits of the proposed approach in our computational results presented in Section 5.

5. NUMERICAL RESULTS

We summarize, in Section 5.1, the computational results for the motivating example from Section 2; a more challenging model problem involving flow through porous media is considered in Section 5.2.

5.1 Results for the Analytic Test Problem

We consider the example from Section 5.1 and study $P_{\bar{\tau}}$ with $\bar{\tau}=3$. To establish a baseline for the values of the Sobol' indices of $P_{\bar{\tau}}(\xi)$, we compute the total order Sobol' indices directly from Eq. (5) using Saltelli sampling. The reference Sobol' indices are computed with 10^6 samples for each of the conditional terms; convergence was numerically verified. We plot the reference total indices in Fig. 2 for comparison. We now compare the reference indices with those obtained through the PCE surrogate when $P_{\bar{\tau}}(\xi)$ is computed analytically using Eq. (5). We allocate 10^3 samples of $P_{\bar{\tau}}(\xi)$ each for the Saltelli sampling method and sparse regression PCE method. The Saltelli method requires N(d+1) samples [51] and so we divide the budget of 10^3 samples equally among each conditional term. Each PCE coefficient can be estimated using the full set of 10^3 samples. For a fair comparison, we use Latin hypercube sampling for both the PCE and Saltelli method. We also use a total PCE order of 3 and the penalty parameter $\lambda=5\times10^{-2}$. Given that the set of total indices is computed, in each method, using a finite number of samples, each index is a random variable with an associated distribution. We compare the standard deviation of each total index for the two GSA methods. In each case, we compute 10^3 realizations of the full set of total indices and compare their respective standard deviations in Fig. 2.

Figure 2 illustrates the higher accuracy, or lower variance, of PCE with sparse regression over Saltelli sampling: the standard deviation of the largest Sobol' index is roughly 3 times smaller with sparse regression than it is with Saltelli sampling. This gap in accuracy appears to diminish for smaller indices, although the methods do not show comparable accuracy until the indices are below 0.1. As $P_{\bar{\tau}}$ can be expressed analytically, there may be additional benefits of the sparse regression method to be seen when one considers performing GSA on a rare event probability with noise due to sampling. We note that the total order of the PCE basis and the penalty parameter λ , which are user-defined parameters, can be changed without the need for additional runs of SS. These parameters can be cross validated in a post-processing step after the rare event simulation step, providing flexibility in this approach without adding any significant computational burden.

When combining PCE-based GSA with SS for estimating $P_{\bar{\tau}}(\xi)$, there is a trade-off between the inner loop cost of estimating $P_{\bar{\tau}}$ via SS and the outer loop of aggregating $P_{\bar{\tau}}$ samples to build the PCE. In Fig. 3, we separately vary $N_{\rm SS}$ and $N_{\rm SAMP}$ and examine the resulting distribution of the total Sobol' indices, computed via sparse regression

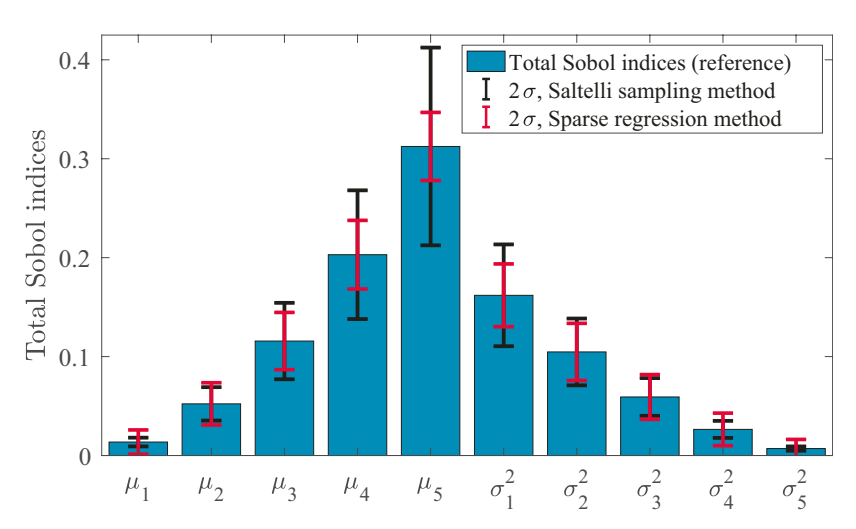


FIG. 2: Total Sobol' indices of $P_{\bar{\tau}}$, with $\bar{\tau}=3$, from Eq. (5); the error bars illustrate the variability of the two sampling methods (Saltelli sampling and sparse regression PCE) around the reference values

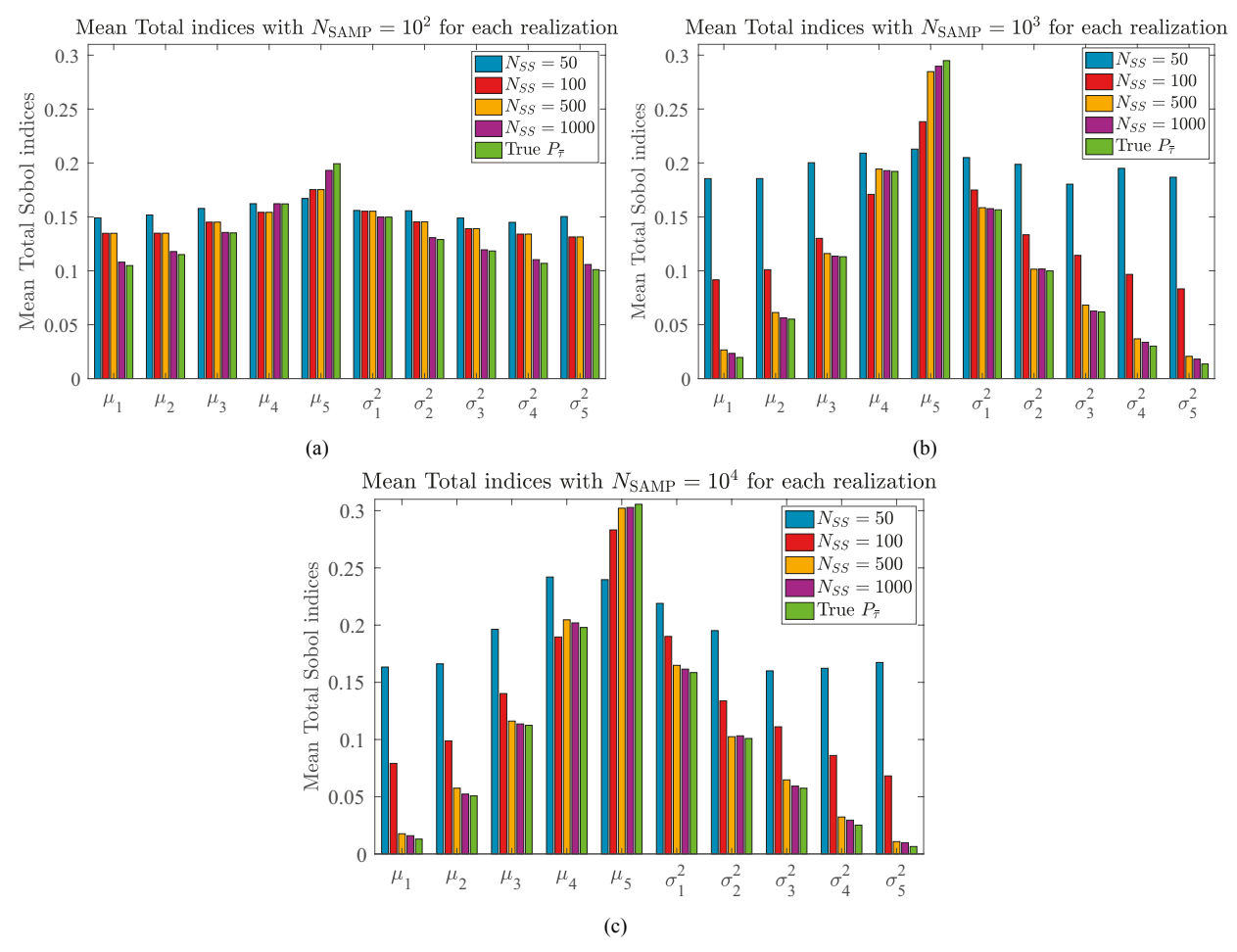


FIG. 3: Mean Total Sobol' indices, varying the computational cost of SS and the PCE construction. Each plot varies N_{SAMP} and each colored bar varies N_{SS} , with the final bar of each index corresponding to the analytic $P_{\bar{\tau}}$.

PCE. For a fixed $N_{\rm SAMP}$, we compute multiple realizations of the total indices for several values of $N_{\rm SS}$. Figure 3(a) displays the expected value of the total indices for $N_{\rm SAMP}=100$. Regardless of how accurately we estimate P_{τ} , the indices do not approach their true values because the PCE is built using an inadequate number of samples, resulting in a poor surrogate. By contrast, Fig. 3(b) shows that for $N_{\rm SAMP}=10^3$, we only need a modest $N_{\rm SS}$ to approximate the Sobol' indices. Indeed, for $N_{\rm SS}=500$, we are able to resolve the total indices very well. We also examine the case of $N_{\rm SAMP}=10^4$ in Fig. 3(c). Again, we are able to resolve the total indices well using only $N_{\rm SS}=500$ and are able to achieve the correct ordering for as little as $N_{\rm SS}=100$.

These results indicate that (i) a modest number of samples allocated to SS is enough to get a rough estimate of $P_{\bar{\tau}}$ and (ii) a moderate number of realizations of $P_{\bar{\tau}}(\xi)$ is then sufficient for accurate GSA. In other words, given rather poor estimations of $P_{\bar{\tau}}$, we are still able to extract accurate GSA results, due to the fact that the sparse regression technique is robust to noisy QoI evaluations.

5.2 Subsurface Flow Application

We consider the equations for single-phase, steady-state flow in a square domain $\mathcal{D} = [0, 1]^2$:

$$-\nabla \cdot \left(\frac{\kappa}{\mu} \nabla p\right) = 0 \quad \text{in } \mathcal{D},$$

$$p = 1 \quad \text{on } \Gamma_1,$$

$$p = 0 \quad \text{on } \Gamma_2,$$

$$\nabla p \cdot n = 0 \quad \text{on } \Gamma_3,$$

$$(16)$$

where κ is the permeability, μ is the viscosity, and p is the pressure. The boundaries Γ_1 , Γ_2 , and Γ_3 indicate the left boundary, the right boundary, and the top/bottom boundaries, respectively. The Darcy velocity is defined as $v = -(\kappa/\mu)\nabla p$. In the present study, we let $\mu = 1$. The source of uncertainty in this problem is in the permeability field, which we model as a random field. We consider the flow of particles through the medium and focus on determining the probability that said particles do not reach the outflow boundary in a given amount of time. This problem has been used previously as a test problem for rare event estimation in [1] as it pertains to the long-term reliability of nuclear waste repositories. Our goal is to perform GSA with respect to the hyper-parameters that define the distribution law of the permeability field.

5.3 The Statistical Model for the Permeability Field

Following standard practice [1,52], we model the permeability field as a log-Gaussian random field:

$$\log \kappa(x, \mathbf{\omega}) = a(x, \mathbf{\omega}) = \bar{a}(x) + \sigma_a z(x, \mathbf{\omega}), \tag{17}$$

where $x \in \mathcal{D}$ and ω belongs to sample space that carries the random process. Here, \bar{a} is the mean of the random field, σ_a is a scalar which controls the pointwise variance of the field, and z is a centered (zero-mean) random process. We let the covariance function of z be given by

$$c_z(x,y) = \exp\left(-\frac{|x_1 - y_1|}{\ell_x} - \frac{|x_2 - y_2|}{\ell_y}\right), \quad x, y \in \mathcal{D},$$
 (18)

where ℓ_x and ℓ_y denote the correlation lengths in horizontal and vertical directions. The random field is represented via a truncated Karhunan-Loève expansion (KLE):

$$a(x, \mathbf{\omega}) \approx \bar{a}(x) + \sum_{k=1}^{N_{KL}} \sqrt{\lambda_k} \, \theta_k(\mathbf{\omega}) \, e_k(x).$$
 (19)

In this representation, $\theta_1, \dots, \theta_{N_{KL}}$ are independent standard normal random variables and (λ_i, e_k) , $k = 1, \dots, N_{KL}$, are the leading eigenpairs of the covariance operator of the process. Our setup for the uncertain log-permeability

field follows the one in [52]: we use permeability data from the Society for Petroleum Engineers [53] to define \bar{a} . Once we truncate the KLE, the random vector $\boldsymbol{\theta} = [\theta_1 \quad \theta_2 \quad \dots \quad \theta_{N_{KL}}]^{\top}$ fully describes the uncertainty in the log-permeability field.

To ensure that the KLE accurately models the variability of the infinite-dimensional field, we examine the eigenvalue decay of the covariance operator with the goal to truncate the KLE so that at least 90% of the average variance of the field is maintained. For $\ell_x = \ell_y = 0.4$, which are the smallest correlation lengths considered in the present study, we require at least $N_{KL} = 126$. The number of retained KL modes then determines the dimensionality of the rare event estimation problem, and is henceforth fixed at 126. The dimension independent properties of SS are advantageous in this regime.

For illustration, we plot two realizations of the random field, with the corresponding pressure and velocity fields obtained by solving the governing PDE (16), in Fig. 4. In our computations, we solve the PDE using piecewise linear finite elements in MATLAB's finite element toolbox with 50 mesh points in each direction.

5.4 The Qol and Rare Events under Study

The position x of a particle moving with the flow through the medium is determined by the following ODE,

$$\frac{d\mathbf{x}}{dt} = \mathbf{v},
\mathbf{x}(0) = \mathbf{x}_0,$$
(20)

where v is the Darcy velocity. We consider a single particle with initial position at $x_0 = \begin{bmatrix} 0 \\ 0.5 \end{bmatrix}$. The solution x of Eq. (20) depends not only on time but also on θ due to dependence of v on θ , i.e., $x = x(t, \theta)$. We take the QoI q as the hitting time, i.e., the time it takes a particle to travel through the medium from left to right:

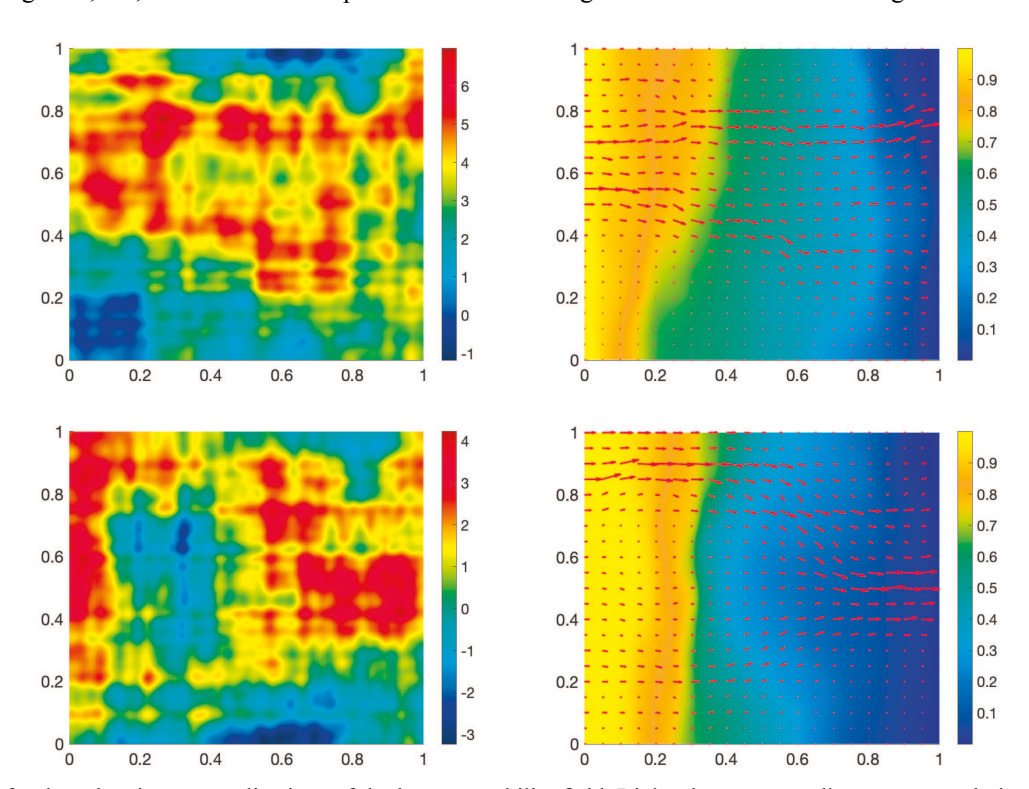


FIG. 4: Left: plots showing two realizations of the log permeability field. Right: the corresponding pressure solution and arrows indicating the resulting Darcy velocity field.

$$q(\mathbf{\Theta}) = \{t : x_1(t, \mathbf{\Theta}) = 1\}.$$

We aim to determine the rare event probability $P_{\bar{\tau}} = \mathbb{P}(q > \bar{\tau})$. The parameters ℓ_x , ℓ_y , and σ_a parametrize the uncertainty in the permeability field; we consider them as hyper-parameters and set $\xi = [\ell_x \quad \ell_y \quad \sigma_a]^{\top}$. We set the nominal values of the hyper-parameters $\xi_{nom} = [0.4 \quad 0.4 \quad 0.8]^{\top}$. We simulate realizations of the permeability field at these nominal hyper-parameters and plot the distribution of q. Each of these realizations requires one PDE solve and one ODE solve. As illustrated in Fig. 5, the distribution for q corresponds to a heavy-tailed distribution. We select as the threshold $\bar{\tau} = 4.5$ and consider quantifying the sensitivity of $P_{\bar{\tau}}(\xi)$ with respect to the hyper-parameters defining the KLE.

5.5 Rare Event Probabilities and GSA

In our first set of experiments, we use SS with $N_{\rm SS}=10^3$ samples per intermediate level; each of these samples corresponds to one solution of the full subsurface flow problem, including a PDE and ODE solve. For each evaluation of SS, approximately five intermediate levels are used, resulting in approximately 5×10^3 function evaluations. Our hyper-parameters are drawn from a uniform distribution centered at ξ_{nom} with a spread of plus or minus 10% of ξ_{nom} . We use these SS estimations of $P_{\bar{\tau}}(\xi)$ in order to build the corresponding PCE surrogate, where the polynomial basis is truncated at a total polynomial order of 5. Note the decision of where to truncate the PCE basis does not need to be made prior to estimating the set of $P_{\bar{\tau}}(\xi)$ samples.

The samples for the hyper-parameters are drawn using a Latin hypercube sampling scheme. We use 10^3 estimations of $P_{\bar{\tau}}(\xi)$ to construct the PCE surrogate. Again, we use sparse regression to recover the PCE coefficients, while promoting sparsity in the set of PCE coefficients, and so mitigate the effects of noise induced by SS. In Fig. 6, we use two different values of λ when promoting sparsity in order to illustrate the effect of λ on the results. Note that when λ is made smaller, the PCE coefficients decrease in magnitude, promoting a sparser PCE spectrum. In both cases, the ordering of the total Sobol' indices remains consistent and, thus, conclusions with respect to parameter sensitivity are unaffected. For this experiment, we therefore conclude that choosing λ by trial and error is sufficient. Should one encounter a scenario where the GSA results are more sensitive to λ , more systematic approaches are possible [46,48].

We lastly return to the key point made in Section 5.1, that the proposed method is capable of producing reliable GSA results, while using a modest number of inner and outer loop samples (N_{SS} and N_{SAMP} , respectively). In Fig. 7, we report results corresponding to $N_{SS} = 500$. In the left panel of the figure we study the effect of N_{SAMP} on the PDF of the PCE surrogate. In the right panel, we plot the Sobol' indices corresponding to each of the computed surrogates. The results in Fig. 7 should also be compared with those in Fig. 6, where larger values of N_{SS} and N_{SAMP} were used. This experiment indicates that $P_{\overline{\tau}}$ and the Sobol' indices themselves can be well-approximated with a

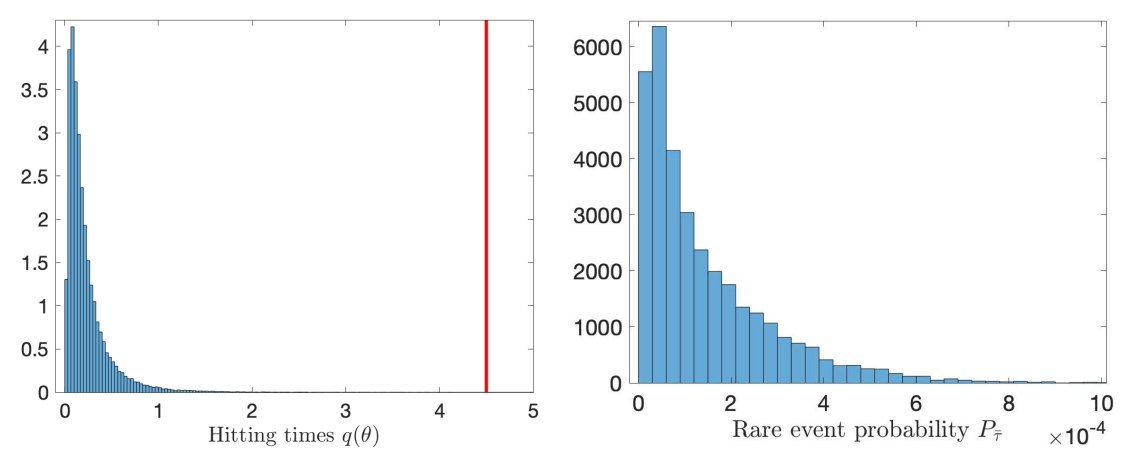


FIG. 5: Left: Histogram of q for nominal hyper-parameters. Vertical line indicates rare event threshold of $\bar{\tau} = 4.5$. Right: histogram of the rare event probability, estimated via SS with uniformly distributed hyper-parameters.

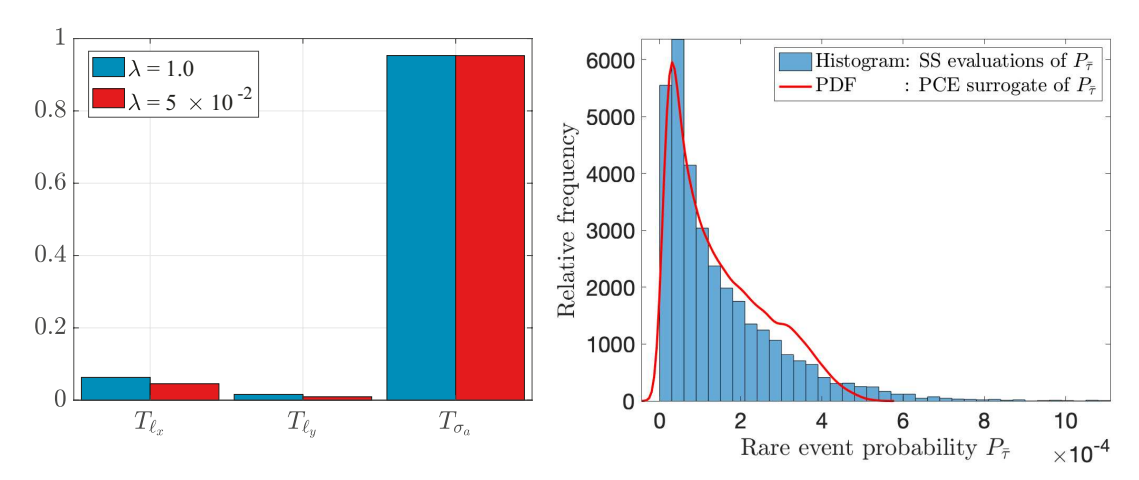


FIG. 6: Left: total Sobol' indices for $P_{\bar{\tau}}(\xi)$ computed from recovered PCE coefficients; results are reported with regularization constant $\lambda=1$ and $\lambda=5\times10^{-2}$. Right: PDF of PCE surrogate compared with $P_{\bar{\tau}}$ evaluation histogram. $N_{SAMP}=10^4$ is used for better resolution of distributions.

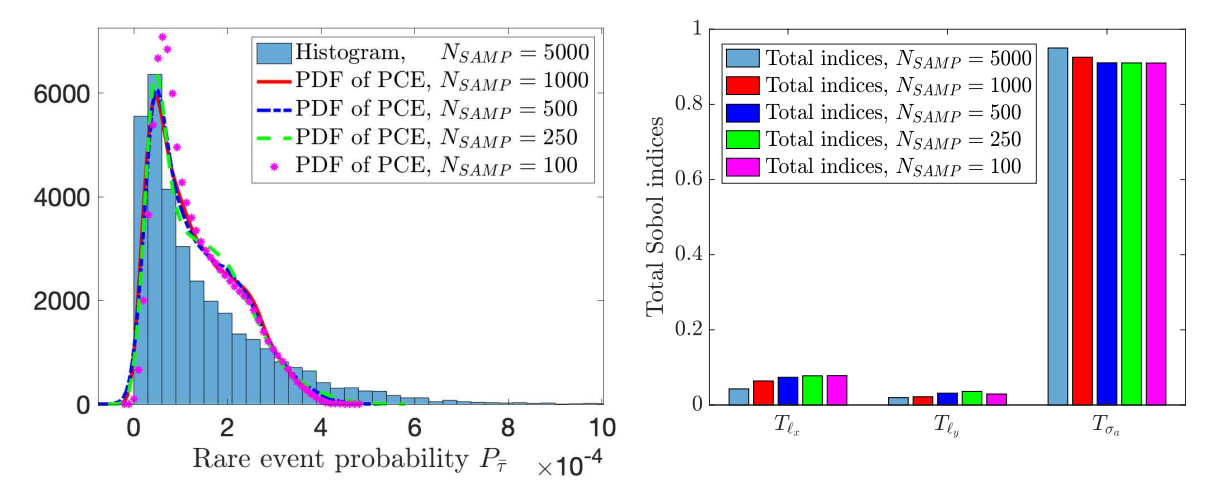


FIG. 7: Distributions of $P_{\bar{\tau}}$ for $N_{SS} = 500$ and varying values of N_{SAMP} . For each N_{SAMP} , we build the PCE surrogate and approximate its PDF with 10^5 samples. The set of $P_{\bar{\tau}}$ samples used for differing N_{SAMP} is nested within sets of larger samples. Corresponding total indices are included, computed directly from the PCE surrogates.

modest number of samples in both the inner and outer loops. In this case, using both N_{SS} and N_{SAMP} on the order of 10^2 is sufficient for obtaining accurate GSA results. The combined cost of this method is thus reduced by a significant margin compared with the similar results in Fig. 6. The efficiency gains of this method indicate the potential for deployment on problems which would otherwise be intractable.

6. CONCLUSION AND FUTURE WORK

We have shown that the feasibility of the standard double-loop approach for GSA of rare event probabilities can be significantly extended beyond simple applications. This requires appropriate acceleration methods; in our case, this is achieved through subset simulation and the choice of a surrogate model allowing for the analytical calculation of Sobol' indices. This approach is conceptually simple and does not require the development of new, *ad hoc* sensitivity concepts. While we have extended the range of applicability of the double-loop approach, we acknowledge that more research is needed to deal with computationally expensive, high-dimensional problems.

The efficiency of our method crucially depends on working with surrogate models for which sensitivity measures —here, Sobol' indices—can be computed cheaply or "for free"; this clearly and strongly limits the type of GSA which can be carried out by the approach. More generally, if q is the original QoI and if \tilde{q} is the resulting QoI for a given surrogate model, more work is needed to understand the relationship between the approximation error $q - \tilde{q}$ and the resulting GSA error $\mathcal{S}(q) - \mathcal{S}(\tilde{q})$ where $\mathcal{S}(\cdot)$ is some sensitivity measure; more explicitly, there may be room for the development of "cheap" surrogate models with moderate approximation errors and *small* GSA errors. Additionally, both our sensitivity analysis method as well as surrogate modeling approach rely on the assumption that the hyper-parameters are independent. In some cases one might be interested in GSA of rare event probabilities to both hyper-parameters and additional parameters in a model that might be uncertain and possibly correlated. Therefore, another interesting line of inquiry is to consider GSA of rare event probability with respect to correlated parameters. Further study may also include extensions of our approach to other moment-based QoIs (e.g., cumulative distribution function approximation, skewness, kurtosis) and the use of perturbation-based methods for GSA [23] as opposed to considering a discrete set of hyper-parameters.

ACKNOWLEDGMENTS

This research was supported by NSF through Grant Nos. DMS 1745654 and DMS 1953271 and the U.S. Department of Energy (DOE) through Sandia National Laboratories.

REFERENCES

- 1. Ullmann, E. and Papaioannou, I., Multilevel Estimation of Rare Events, SIAM/ASA J. Uncertainty Quantif., 3(1):922–953, 2015.
- 2. Tong, S., Vanden-Eijnden, E., and Stadler, G., Extreme Event Probability Estimation Using PDE-Constrained Optimization and Large Deviation Theory, with Application to Tsunamis, *Commun. Appl. Math. Comput. Sci.*, **16**(2):181–225, 2021.
- 3. Beck, J.L. and Zuev, K.M., Rare-Event Simulation, in *Handbook of Uncertainty Quantification*, R. Ghanem, D. Higdon, and H. Owhadi, Eds., Cham, Switzerland: Springer, pp. 1075–1100, 2017.
- 4. Morio, J., Influence of Input PDF Parameters of a Model on a Failure Probability Estimation, *Simul. Modell. Practice Theory*, **19**(10):2244–2255, 2011.
- 5. Sobol', I.M., On Sensitivity Estimation for Nonlinear Mathematical Models, Mat. Model., 2(1):112–118, 1990.
- 6. Sobol', I.M., Sensitivity Estimates for Nonlinear Mathematical Models, Math. Modell. Comput., 1:407–414, 1993.
- 7. Sobol', I.M., Global Sensitivity Indices for Nonlinear Mathematical Models and Their Monte Carlo Estimates, *Math. Comput. Simul.*, **55**:271–280, 2001.
- 8. Owen, A., Better Estimation of Small Sobol' Sensitivity Indices, ACM Trans. Model. Comput. Simul., 23:11-1-11-17, 2013.
- 9. Ashraf, M., Oladyshkin, S., and Nowak, W., Geological Storage of CO₂: Application, Feasibility and Efficiency of Global Sensitivity Analysis and Risk Assessment Using the Arbitrary Polynomial Chaos, *Int. J. Greenhouse Gas Control*, **19**:704–719, 2013.
- 10. Sochala, P. and Le Maître, O., Polynomial Chaos Expansion for Subsurface Flows with Uncertain Soil Parameters, *Adv. Water Res.*, **62**:139–154, 2013.
- 11. Guo, L., Fahs, M., Hoteit, H., Gao, R., and Shao, Q., Uncertainty Analysis of Seepage-Induced Consolidation in a Fractured Porous Medium, *Comput. Model. Eng. Sci.*, **129**(1):279–297, 2021.
- 12. Alexanderian, A., Winokur, J., Sraj, I., Srinivasan, A., Iskandarani, M., Thacker, W.C., and Knio, O.M., Global Sensitivity Analysis in an Ocean General Circulation Model: A Sparse Spectral Projection Approach, *Comput. Geosci.*, **16**(3):757–778, 2012.
- 13. Sraj, I., Mandli, K.T., Knio, O.M., Dawson, C.N., and Hoteit, I., Uncertainty Quantification and Inference of Manning's Friction Coefficients Using DART Buoy Data during the Tohoku Tsunami, *Ocean Modell.*, **83**:82–97, 2014.
- 14. Navarro Jimenez, M., Le Maître, O., and Knio, O., Global Sensitivity Analysis in Stochastic Simulators of Uncertain Reaction Networks, *J. Chem. Phys.*, **145**(24):244106, 2016.
- 15. Hantouche, M., Sarathy, S.M., and Knio, O.M., Global Sensitivity Analysis of n-Butanol Reaction Kinetics Using Rate Rules, *Combust. Flame*, **196**:452–465, 2018.

- 16. Merritt, M., Alexanderian, A., and Gremaud, P.A., Multiscale Global Sensitivity Analysis for Stochastic Chemical Systems, *Multiscale Model. Simul.*, **19**(1):440–459, 2021.
- 17. Olivares, A. and Staffetti, E., Uncertainty Quantification of a Mathematical Model of COVID-19 Transmission Dynamics with Mass Vaccination Strategy, *Chaos, Solitons Fractals*, **146**:110895, 2021.
- 18. Lu, X. and Borgonovo, E., Global Sensitivity Analysis in Epidemiological Modeling, Eur. J. Oper. Res., in press, 2021.
- 19. Hart, J., Gremaud, P., and David, T., Global Sensitivity Analysis of High-Dimensional Neuroscience Models: An Example of Neurovascular Coupling, *Bull. Math. Biol.*, **81**(6):1805–1828, 2019.
- 20. Saltelli, A., Ratto, M., Andres, T., Campolongo, F., Cariboni, J., Gatelli, D., Saisana, M., and Tarantola, S., *Global Sensitivity Analysis: The Primer*, New York: Wiley, 2008.
- 21. Iooss, B. and Lemaître, P., A Review on Global Analysis Methods, in Uncertainty Management in Simulation-Optimization of Complex Systems, G. Dellino and C. Meloni, Eds., Chapter 5, Berlin: Springer, pp. 101–122, 2015.
- 22. Chabridon, V., Balesdent, M., Bourinet, J.M., Morio, J., and Gayton, N., Reliability-Based Sensitivity Estimators of Rare Event Probability in the Presence of Distribution Parameter Uncertainty, *Reliab. Eng. Syst. Saf.*, 178:164–178, 2018.
- 23. Lemaître, P., Sergienko, E., Arnaud, A., Bousquet, N., Gamboa, F., and Iooss, B., Density Modification-Based Reliability Sensitivity Analysis, *J. Stat. Comput. Simul.*, **85**(6):1200–1223, 2015.
- 24. Dupuis, P., Katsoulakis, M.A., Pantazis, Y., and Rey-Bellet, L., Sensitivity Analysis for Rare Events Based on Rényi Divergence, *Ann. Appl. Probab.*, **30**(4):1507–1533, 2020.
- 25. Ehre, M., Papaioannou, I., and Straub, D., A Framework for Global Reliability Sensitivity Analysis in the Presence of Multi-Uncertainty, *Reliab. Eng. Syst. Saf.*, **195**:106726, 2020.
- 26. Wang, Z. and Jia, G., Augmented Sample-Based Approach for Efficient Evaluation of Risk Sensitivity with Respect to Epistemic Uncertainty in Distribution Parameters, *Reliab. Eng. Syst. Saf.*, 197:106783, 2020.
- 27. Wang, P., Li, C., Liu, F., and Zhou, H., Global Sensitivity Analysis of Failure Probability of Structures with Uncertainties of Random Variable and Their Distribution Parameters, *Eng. Comput.*, **126**:1–19, 2021.
- 28. Chabridon, V., Reliability-Oriented Sensitivity Analysis under Probabilistic Model Uncertainty—Application to Aerospace Systems, PhD, Université Clermont Auvergne, 2018.
- 29. Šehić, K. and Karamehmedović, M., Estimation of Failure Probabilities via Local Subset Approximations, *Stat. Comput.*, arXiv:2003.05994, 2020.
- 30. Papaioannou, I., Betz, W., Zwirglmaier, K., and Straub, D., MCMC Algorithms for Subset Simulation, *Probab. Eng. Mech.*, 41:89–103, 2015.
- 31. Bhatia, R. and Davis, C., A Better Bound on the Variance, Am. Math. Mon., 107(4):353–357, 2000.
- 32. Au, S.K. and Beck, J.L., Estimation of Small Failure Probabilities in High Dimensions by Subset Simulation, *Probab. Eng. Mech.*, **16**(4):263–277, 2001.
- 33. Schuëller, G., Pradlwarter, H., and Koutsourelakis, P.S., A Critical Appraisal of Reliability Estimation Procedures for High Dimensions, *Probab. Eng. Mech.*, **19**(4):463–474, 2004.
- 34. Zuev, K.M., Beck, J.L., Au, S.K., and Katafygiotis, L.S., Bayesian Post-Processor and Other Enhancements of Subset Simulation for Estimating Failure Probabilities in High Dimensions, *Comput. Struct.*, **92**:283–296, 2012.
- 35. Melchers, R.E. and Beck, A.T., Structural Reliability Analysis and Prediction, New York: John Wiley & Sons, 2018.
- 36. Peherstorfer, B., Kramer, B., and Willcox, K., Combining Multiple Surrogate Models to Accelerate Failure Probability Estimation with Expensive High-Fidelity Models, *J. Comput. Phys.*, **341**:61–75, 2017.
- 37. Li, J. and Xiu, D., Evaluation of Failure Probability via Surrogate Models, J. Comput. Phys., 229(23):8966–8980, 2010.
- 38. Li, J., Li, J., and Xiu, D., An Efficient Surrogate-Based Method for Computing Rare Failure Probability, *J. Comput. Phys.*, **230**(24):8683–8697, 2011.
- 39. Butler, T. and Wildey, T., Utilizing Adjoint-Based Error Estimates for Surrogate Models to Accurately Predict Probabilities of Events, *Int. J. Uncertainty Quantif.*, **8**(2):143–159, 2018.
- 40. Bourinet, J.M., Rare-Event Probability Estimation with Adaptive Support Vector Regression Surrogates, *Reliab. Eng. Syst. Saf.*, **150**:210–221, 2016.
- 41. Ebeida, M.S., Mitchell, S.A., Swiler, L.P., Romero, V.J., and Rushdi, A.A., Pof-Darts: Geometric Adaptive Sampling for Probability of Failure, *Reliab. Eng. Syst. Saf.*, **155**:64–77, 2016.

42. Bichon, B.J., McFarland, J.M., and Mahadevan, S., Efficient Surrogate Models for Reliability Analysis of Systems with Multiple Failure Modes, *Reliab. Eng. Syst. Saf.*, **96**(10):1386–1395, 2011.

- 43. Le Maître, O. and Knio, O.M., Spectral Methods for Uncertainty Quantification: With Applications to Computational Fluid Dynamics, Berlin: Springer Science & Business Media, 2010.
- 44. Crestaux, T., Le Maître, O., and Martinez, J.M., Polynomial Chaos Expansion for Sensitivity Analysis, *Reliab. Eng. Syst. Saf.*, **94**(7):1161–1172, 2009.
- 45. Asmussen, S. and Glynn, P.W., Stochastic Simulation: Algorithms and Analysis, Vol. 57, Berlin: Springer Science & Business Media, 2007.
- 46. Blatman, G. and Sudret, B., Efficient Computation of Global Sensitivity Indices Using Sparse Polynomial Chaos Expansions, *Reliab. Eng. Syst. Saf.*, **95**(11):1216–1229, 2010.
- 47. Fajraoui, N., Marelli, S., and Sudret, B., Sequential Design of Experiment for Sparse Polynomial Chaos Expansions, SIAM/ASA J. Uncertainty Quantif., 5(1):1061–1085, 2017.
- 48. Hampton, J. and Doostan, A., Compressive Sampling Methods for Sparse Polynomial Chaos Expansions, in *Handbook of Uncertainty Quantification*, R. Ghanem, D. Higdon, and H. Owhadi, Eds., Springer International Publishing, pp. 827–855, 2017
- 49. van den Berg, E. and Friedlander, M.P., SPGL1: A Solver for Large-Scale Sparse Reconstruction, from https://friedlander.io/spg11, 2019.
- 50. Alexanderian, A., On Spectral Methods for Variance Based Sensitivity Analysis, *Probab. Surv.*, 10:51–68, 2013.
- 51. Saltelli, A., Annoni, P., Azzini, I., Campolongo, F., Ratto, M., and Tarantola, S., Variance Based Sensitivity Analysis of Model Output. Design and Estimator for the Total Sensitivity Index, *Comput. Phys. Commun.*, **181**:259–270, 2010.
- 52. Cleaves, H.L., Alexanderian, A., Guy, H., Smith, R.C., and Yu, M., Derivative-Based Global Sensitivity Analysis for Models with High-Dimensional Inputs and Functional Outputs, *SIAM J. Sci. Comput.*, **41**(6):A3524–A3551, 2019.
- 53. SPE International, SPE Comparative Solution Project: Description of Model 2, from https://www.spe.org/web/csp/datasets/set02.htm, 2001.